Effect of Long-Range Correlations on Transport Phenomena in Disordered Media

Muhammad Sahimi
Dept. of Chemical Engineering, University of Southern California, Los Angeles, CA 90089
HLRZ Supercomputer Center, % KFA Jülich, Postfach 1913, 52425 Jülich, Germany

Three different flow and transport phenomena considered here are hydrodynamic dispersion in heterogeneous porous media and aquifers, transport of passive particles in an oscillating flow field, and miscible displacement processes in heterogeneous reservoirs. At microscales all three phenomena are described by the classical convective-diffusion equation (CDE). The presence of long-range correlations at macroscales gives rise to a rich variety of phenomena that cannot be predicted by analyzing the CDE by classical methods. In particular, a new percolation model with long-range correlations provides a rational explanation for the hitherto unexplained field-scale experimental data for hydrodynamic dispersion in porous media and aquifers. Moreover, for transport in oscillating flow in convection cells percolation provides a novel relation between the dispersion coefficient and the Péclet number that cannot be predicted by other methods.

Introduction

Transport in disordered media is relevant to modeling a wide variety of phenomena in natural and industrial processes. Its applications include flow, dispersion and displacement processes in porous media (Sahimi (1993b)), transport of passive particles in random flow fields, diffusion through biological tissues, and transport, mechanical and rheological properties of disordered materials such as polymers, glasses and powders.

Many transport processes in disordered media involve a *critical point*, an example being displacement of oil by water in a porous medium. During this process the permeability of that portion of the pore space that is filled with water is zero, so long as the water phase is not sample spanning. Only when the water-filled pores form sample-spanning paths does the permeability of the water phase become nonzero. In this and similar phenomena, the interplay between the transport or flow process and the disordered structure of the medium gives rise to a rich variety of complex phenomena. Transport processes in disordered media that are accompanied by such critical points are usually modeled as a percolation process in a random medium (for an introduction to percolation see Stauffer and Aharony, 1992, and for its applications see Sahimi, 1994). A percolation system provides one of the simplest prototypes of a disordered medium. In such a system, one inserts at random elementary geometrical objects such as spheres, circles, and sticks in a continuum, or bonds or sites in a network. One then, for example, retains a randomly-selected fraction p of the bonds and deletes the rest of them. The intact bonds represent those regions of the system in which a transport process takes place. For example, in two-phase flow through a porous medium a fraction of the pores may be closed to the flow of one of the fluids because they are occupied by the other fluid. Thus, the interconnectivity of the geometrical objects and the existence of a sample-spanning cluster of them play a fundamental role in the overall transport properties of the system. Moreover, near the critical point percolation exhibits long-range correlations that are similar to those in liquid-vapor phase transitions near a critical temperature. We will discuss this further later in this article.

However, although random percolation has provided much insight into transport in disordered media, natural systems are *not* completely random and usually contain some correlations. In some cases, such as packing of solid particles, there are only short-range correlations in which case the fundamental properties of percolation discussed below remain unchanged. In other cases, such as macroscopically heterogeneous porous media and aquifers (see below), there are long-range correlations that give rise to unusual phenomena very different from those in disordered media without correlations. One objective

M. Sahimi is presently at the University of California, Los Angeles, to which correspondence concerning this article should be addressed.

of this article is to investigate transport and percolation in disordered media with long-range correlations, and to demonstrate their relevance to some practical problems.

On the other hand, while the relevance of percolation to phenomena such as two-phase flow in porous media is now clear and well-understood, there are many other transport processes in disordered media to which the relevance of percolation is not obvious at all. An example is single-phase flow and hydrodynamic dispersion in a heterogeneous porous medium. Since one deals with only one fluid phase, it may not be obvious how percolation can play any role. Another example is dispersion of passive particles in a two-dimensional (2-D) steady and incompressible random flow field, characterized by a random stream function $\psi(x, y)$. Here one has streamlines at all levels $h=\psi(x, y)$, where h is a constant, and it is again not clear at all how connectivity and percolation can play any role in this phenomenon. In fact, it is not even clear how connectivity can be *defined* for such a system. In this article we also seek to establish the relevance of percolation to such transport processes. In particular, we demonstrate that single-phase flow and hydrodynamic dispersion in macroscopically heterogeneous porous media represent transport *through* some sort of a percolation system, while transport of passive particles in 2-D incompressible random flow represents transport *around* a percolation system.

In this article we study three different phenomena which are hydrodynamic dispersion and miscible displacement processes in macroscopically heterogeneous porous media and aquifers, and transport of passive particles in a 2-D oscillating flow field. At microscales all three phenomena are described by a convective-diffusion equation (CDE):

$$\frac{\partial C}{\partial t}+\mathrm{v}\cdot\nabla C=D_L\frac{\partial^2 C}{\partial x^2}+D_T\nabla_2^2 C \tag{1}$$

where C is the concentration of the solute at time t, v is the average flow velocity, D_L and D_T are the longitudinal and transverse dispersion coefficients, respectively, and ∇_2^2 denotes the Laplacian in the transverse directions. We show, however, that the presence of long-range correlations at macroscales gives rise to a rich variety of phenomena that cannot be predicted by the analysis of a CDE by classical methods. Moreover, we show that such long-range correlations are essential for explaining field-scale experimental data for a variety of phenomena.

Percolation in Random Networks

In this section we briefly discuss the main ideas of percolation theory that we shall use in the remainder of the article. To facilitate our discussion, we describe percolation in random networks. Later, we consider percolation in disordered continua. Consider a 2-D or 3-D network of interconnected bonds in which a randomly selected fraction p of the bonds are open to transport. We assign non-zero conductances to these bonds and call them the conducting bonds. The rest of the bonds are closed to any transport process (their conductance is zero). As is well-known, for $p>p_c$ a sample-spanning cluster of conducting bonds is formed and macroscopic transport takes place, where p_c is called the *bond percolation threshold*, which depends on the topology of the network and its dimensionality d. For example, for the square network $p_c=1/2$. An important feature of percolation systems is their *universal* properties near p_c. For example, one can define a correlation length ξ which diverges as $p\to p_c$ according to the power law:

$$\xi\sim(p-p_c)^{-\nu}. \tag{2}$$

The correlation length is the length scale for macroscopic homogeneity of the system. For any length scale $L\gg\xi$, the system is macroscopically homogeneous, and thus the classical transport equations, such as the CDE, are applicable, while for $L\ll\xi$ the system is not homogeneous and such equations are not applicable. Near p_c, the fraction X^A of conducting bonds that are in the sample-spanning cluster vanishes as:

$$X^A\sim(p-p_c)^{\beta}\sim\xi^{-\beta/\nu}. \tag{3}$$

For $L\ll\xi$ the sample-spanning cluster is a self-similar and fractal object with a fractal dimension $d_p=d-\beta/\nu$. Another important property of the sample-spanning cluster relevant to our study is its outer perimeter or *hull*. This is defined as the number of empty sites (those that are not connected to any conducting bonds) that (1) are adjacent to the cluster, and (2) can be connected to "infinity" by a path of empty sites connected as either nearest or next-to-nearest neighbors. Figure 1 shows the hull of a 2-D percolation cluster. For any $L\ll\xi$ the hull is also a fractal object, and Saleur and Duplantier (1987) showed that in 2-D:

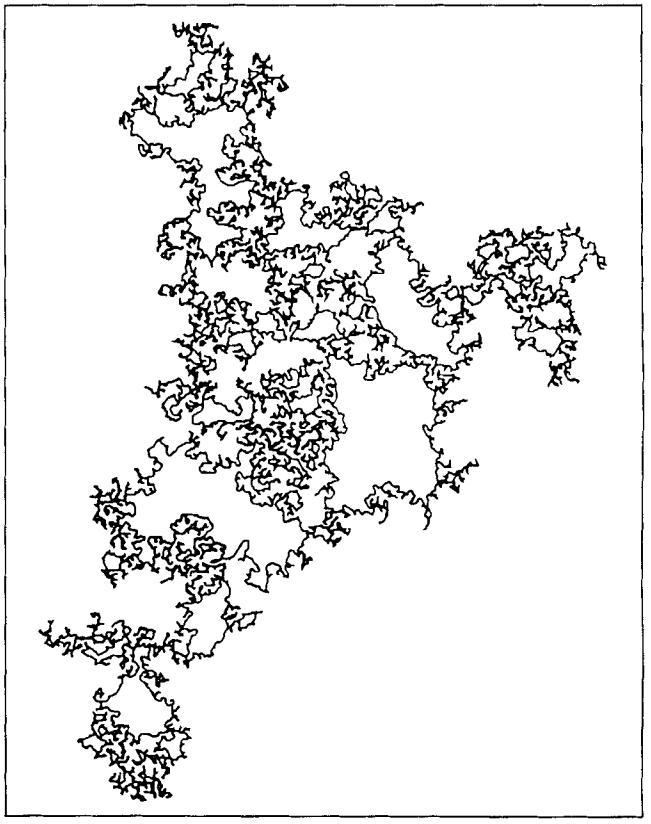

Figure 1. Outer perimeter or hull of a 2-D percolation cluster.

Table 1. Currently-Accepted Values of Critical Exponents and Fractal Dimensions in d-Dimensions*

d	β	ν	β_B	d_p	d_b	d_h	μ	e
2	5/36	4/3	0.48	91/48	1.64	7/4	1.3	1.3
3	0.41	0.88	1.05	2.52	1.87	2.52	2.0	2.0

*Rational or integer numbers represent exact values.

$$d_h = 1 + \frac{1}{\nu}. \tag{4}$$

Monte Carlo simulations of Ziff (1986) are in perfect agreement with Eq. 4. In three dimensions, it can be shown (Strenski et al., 1991) that $d_h = d_p$.

The sample-spanning cluster can be divided into two parts: the dead-end part that carries no flow or current, and the *backbone* which is the multiply-connected part of the cluster, through which flow and transport take place. Near p_c the fraction X^B of the backbone bonds vanishes as:

$$X^B \sim (p - p_c)^{\beta_B} \sim \xi^{-\beta_B/\nu} \tag{5}$$

while for any $L \ll \xi$ the backbone is a fractal object with a fractal dimension $d_b = d - \beta_B/\nu$.

Suppose now that the conductance of the bonds is selected randomly from a distribution function $f(g)$. Then, the macroscopic conductivity G of the system vanishes as $p \to p_c$ according to the power law:

$$G \sim (p - p_c)^{\mu} \sim \xi^{-\mu/\nu}. \tag{6}$$

Similarly, if the network represents the pore space of a porous medium in which a fraction p of the pores are open to flow and diffusion, then a hydrodynamic permeability K and an effective diffusivity D can be defined. Near p_c the permeability vanishes as:

$$K \sim (p - p_c)^{e} \sim \xi^{-e/\nu} \tag{7}$$

whereas it can be shown that as $p \to p_c$ one has:

$$D \sim (p - p_c)^{\mu - \beta} \sim \xi^{-\theta_d} \tag{8}$$

where $\theta_d = (\mu - \beta)/\nu = \mu/\nu + d_p - d$. The exponents ν, β and β_B (and thus d_p, d_h, and d_b) are universal and depend on only d, provided that there are no long-range correlations in the system (see below). Moreover, e and μ are also universal if (Kogut and Straley, 1979; Straley, 1982; Sahimi et al., 1983; Feng et al., 1987) $f(0)$ is not singular, in which case $e = \mu$. Otherwise, e and μ are not in general equal.

Finally, since for $L \ll \xi$, that is, in the fractal regime, the only dominant length scale of the system is L, one should replace ξ by L. Thus, for example, for $L \ll \xi$ Eq. 7 is rewritten as:

$$K \sim L^{-e/\nu}. \tag{9}$$

Therefore, in the fractal regime all physical quantities are *scale dependent*. We point out that fractality of a system implies that there are long-range correlations in the system, up to the upper length scale at which the system can be considered a fractal (which, for percolation, is ξ). Table 1 presents the currently-accepted values of the critical exponents and the fractal dimensions for random percolation in 2-D and 3-D networks.

Fractional Brownian Motion and Correlated Percolation

So far we have discussed percolation in *random* systems. There are many disordered systems whose structure and microscopic properties are not random, but are characterized by short- or long-range correlations in space and/or time. In this section we discuss one stochastic process that gives rise to long-range correlations, and has found many applications in various problems. Consider a stationary stochastic process $B_H(r)$ with the following mean and variance:

$$\langle B_H(r) - B_H(r_0) \rangle = 0 \tag{10}$$

$$\langle [B_H(r) - B_H(r_0)]^2 \rangle \sim |r - r_0|^{2H} \tag{11}$$

where $r = (x, y, z)$ and $r_0 = (x_0, y_0, z_0)$ are two arbitrary points in space, and H is called the Hurst exponent. This stochastic process is called *fractional Brownian motion* (fBm) (Mandelbrot and Van Ness, 1968). A remarkable property of fBm is that it generates correlations whose extent is *infinite*. For example, if we define a correlation function $C(r)$ (where $r = |r|$) by:

$$C(r) = \frac{\langle -B_H(-r) B_H(r) \rangle}{\langle B_H(r)^2 \rangle} \tag{12}$$

then one finds that $C(r) = 2^{2H-1} - 1$, *independent* of r. Moreover, the type of correlations can be tuned by varying H. If $H > 1/2$, then $C(r) > 0$ and fBm displays *persistence*, that is, a trend (for example, a high or low value) at r is likely to be followed by a similar trend at $r + \Delta r$. On the other hand, if $H < 1/2$, then $C(r) < 0$ and fBm generates *antipersistence*, that is, a trend at r is not likely to be followed by a similar trend at $r + \Delta r$. Finally, $C(r)$ vanishes for $H = 1/2$, and $B_H(r)$ is equivalent to an ordinary diffusion process. Thus, varying H allows us to generate correlations or anticorrelations of infinite extent. Figures 2a and 2b show examples of numbers generated by 2-D fBms and their dependence on H. Note that, if instead of Eq. 12 we define the correlation function by the usual relation, $C(r) = \langle B_H(r') B_H(r + r') \rangle$, where $\langle \cdot \rangle$ denotes an average over all r', then it is not difficult to show that:

$$\Delta C = C(0) - C(r) \sim r^{2H}. \tag{13}$$

Equation 13 tells us that in a d-dimensional space the correlations that are generated by an fBm *do not* die out, as long as $H > 0$. An example of such correlations is shown in Figure 3.

A convenient way of representing a distribution function is through its spectral density $S(\omega)$, the Fourier transform of its variance. For an fBm in d-dimensions it can be shown that:

$$S(\omega) \sim \frac{1}{(\sum_{i=1}^{d} \omega_i^2)^{H + d/2}} \tag{14}$$

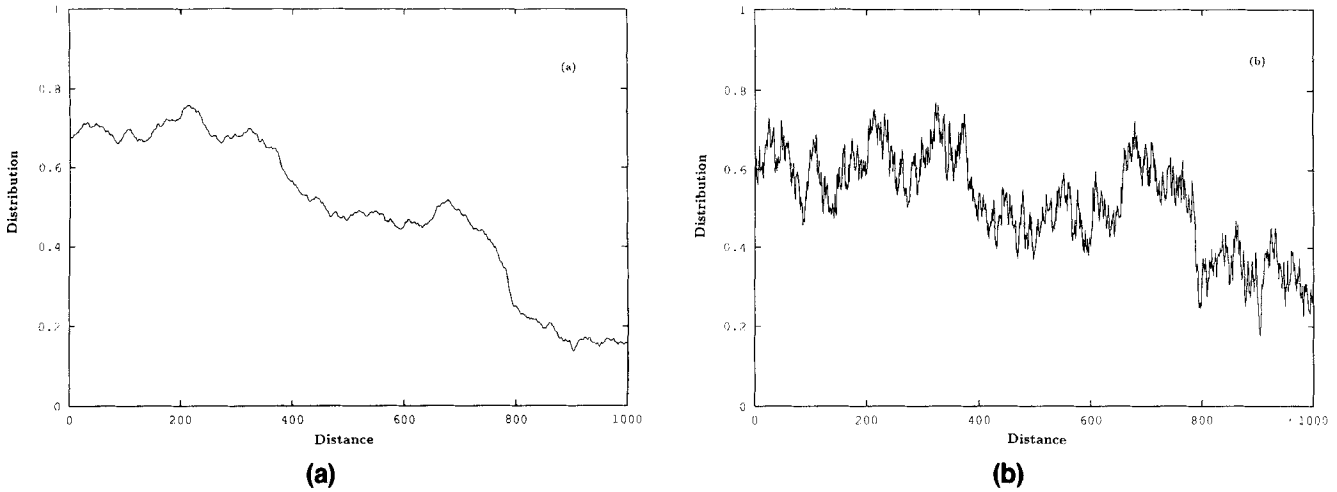

Figure 2. Examples of numbers generated by a 2-D fBm.

(a) $H=0.8$; (b) $H=0.2$.

where $\omega=(\omega_1, \cdots, \omega_d)$. This spectral representation also allows us to introduce a cutoff ξ_{co} such that:

$$S(\omega) \sim \frac{1}{(\xi_{co}+\Sigma_{i=1}^{d}\omega_i^2)^{H+d/2}}. \tag{15}$$

This cutoff allows us to control the length scale over which the spatial properties of a system are correlated (or anticorrelated). Thus, for length scales $l<1/\xi_{co}^{1/2}$ they preserve their correlations (anticorrelations), but for $l>1/\xi_{co}^{1/2}$ they become random and uncorrelated. An example is shown in Figure 4 for $H=0.8$ and $\xi_{co}=100$, which should be compared with Figure 2a which corresponds to $\xi_{co}=0$. Also shown in Figure 3 are the correlation functions for systems in which a cutoff has been introduced. As can be seen, as ξ_{co} increases, that is, as the length scale l over which events or properties are correlated decreases, the correlation function becomes a constant, typical of random processes. The spectral density representation also provides a convenient method for generating a sequence of numbers that obey an fBm using a fast Fourier transform technique. One first generates random numbers, uniformly distributed in (0,1), and assigns them to the sites or bonds of a d-dimensional network. The Fourier transform of the d-dimensional array of the numbers is then calculated. These Fourier-transformed numbers are then multiplied by the square root of the righthand side of Eq. 14 or 15. The results, when inverse Fourier transformed back into the real space, obey an fBm. To avoid the problem associated with the periodicity of the numbers arising as a result of their Fourier transforming, one should generate the array for a much larger network than the actual size that is to be used, and use the central part of the network. This is the method used in this article. The properties of a wide variety of systems have been shown to follow fBm statistics. For example, it has been shown (Hewett, 1986; Hewett and Behrens, 1990) that the permeability of many heterogeneous rock masses follow fBm with $H\simeq 0.75-0.85$. It has also been shown (Peng et al., 1993) that

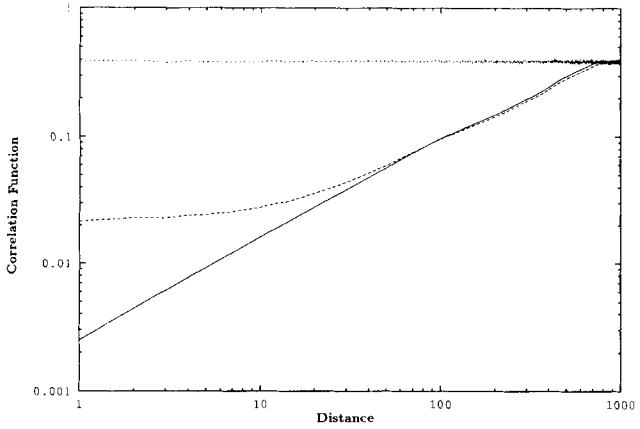

Figure 3. Correlation function defined by Eq. 13 for a 2-D fBm.

The curves correspond, from top to bottom, to $\xi_{co}=1, 10^{-4}$ and 0, respectively.

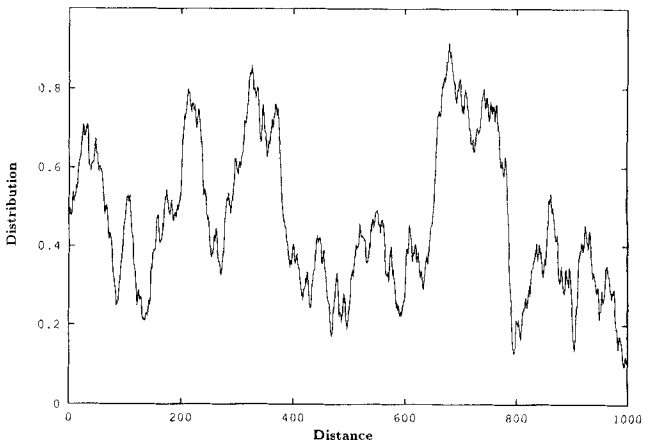

Figure 4. Examples of numbers generated by a 2-D fBm.

$H=0.8$; $\xi_{co}=100$. Compare this with Figure 2a for which $\xi_{co}=0$.

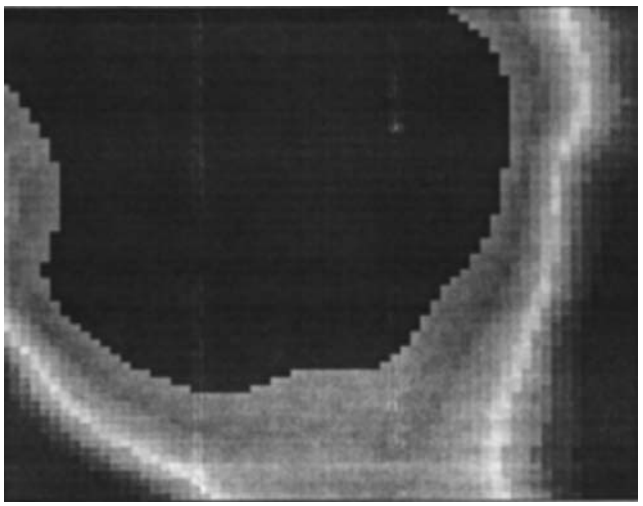

Figure 5. Distribution of bond permeabilities in a square network, generated by an fBm with $H = 0.9$.

Lightest area corresponds to bonds with the largest permeabilities; 50% of the bonds with the lowest permeabilities have been removed, and are shown as the darkest area.

successive increments in the cardiac beat-to-beat intervals of healthy subjects follow fBm with $H < 1/2$.

We now use fBm to develop a percolation process with long-range correlations. In the next section we establish the relevance of this correlated percolation to transport in disordered media. Weinrib and Halperin (1983), Weinrib (1984), and Prakash et al. (1992) have previously proposed models of correlated percolation. However, our model is motivated by Hewett's (1986) analysis of the permeability and porosity of rock formations, and is different from their models. Since the permeability of heterogeneous rock seems to follow an fBm, we propose the following model. To each bond of a network we assign a permeability selected from an fBm with a given H. In random percolation discussed above, the bonds of the network are selected at random and are assigned zero permeability. However, if we follow the same algorithm here, we would again generate a random percolation cluster, because random removal of the bonds would destroy the correlations between the bonds. Instead, we select those bonds that have the *smallest* permeabilities and remove them (we change their permeability to zero). The idea is that since fBm gives rise to a broad distribution of the permeabilities, then a finite fraction of the bonds should have very small permeabilities, and therefore their contribution to the macroscopic permeability would be negligible. Figure 5 shows a square network in which the bond permeabilities have been selected according to an fBm with $H = 0.9$, and 50% of its bonds with the smallest permeabilities have been removed. For comparison, we show in Figure 6 the same network in which the same fraction of the bonds have been removed *at random*. The difference between the two systems is striking, and can be understood by considering the nature of fBm. Since for $H > 0.5$ the correlations are positive, most bonds with large or small permeabilities are clustered together. As a result, removal of the low permeability bonds *does not* generate much randomness in the system, and in fact, as we can see in Figure 5, the percolation cluster that is generated in this process does not have many dead-end bonds, that is, it is very similar to the backbone of the system.

Figure 6. Distribution of bond permeabilities in a square network, generated by an fBm with $H = 0.9$.

Lightest area corresponds to bonds with the largest permeabilities; 50% of the bonds, shown by the darkest area, have been removed *at random*.

We have calculated the critical exponents (see above) that characterize our correlated percolation model for $1/2 \leq H < 1$, the range of interest to us in this article. The methods and details of our calculations are beyond the scope of this article and are given elsewhere (Sahimi and Mukhopadhyay, 1995). For our purpose here it suffices to say that d_p retains its value for random percolation for almost all values of H, except when $H \simeq 1$, in which case $d_p \to d$ as $H \to 1$, that is, the sample-spanning cluster becomes compact. Moreover, we found that d_b is close to d_p, confirming our assertion that for $H > 1/2$ the sample-spanning cluster and its backbone are very similar. For example, we found that in 2-D d_b $(H = 0.6) \simeq 1.82$, compared with $d_p = 91/48 \simeq 1.89$, and $d_b(H = 0.98) = d_p(H = 0.98) \simeq 1.96$. We also found that as $H \to 1$ the exponents e and μ are smooth and decreasing functions of H. For example, we found that in 2-D $\hat{e} = e/\nu \simeq 0.91$ and $\hat{\mu} = \mu/\nu \simeq 0.95$ for $H = 0.6$, and $\hat{e} \simeq 0.76$ and $\hat{\mu} \simeq 0.32$ for $H = 0.98$ (compare these results with those shown in Table 1). Thus, long-range correlations give rise to nonuniversal exponents for percolation. Finally, in the range $1/2 \leq H < 1$, where the correlations are positive, the percolation threshold p_c of the system decreases with increasing H. For example, we found that for the square network $p_c(H = 0.8) \simeq 0.4$, compared with $p_c = 1/2$ for random percolation.

Anomalous Dispersion in Heterogeneous Porous Media

We now show that our correlated percolation method can be used for explaining field-scale experimental data on hydrodynamic dispersion in heterogeneous porous media and aquifers. There have been several field studies of dispersion (for a review see Gelhar et al., 1992) indicating that the longitudinal dispersion coefficient D_L and the corresponding dispersivity $\alpha_L = D_L/v$ are *scale-dependent*. Arya et al. (1988) analyzed over 130 greatly varying dispersivities, collected on length scales up

to 100 km. Although these data show large scatter, their analysis indicated that about 75% of them follow the following scaling law:

$$\alpha_L \sim L_m^{\alpha} \tag{16}$$

where L_m is the length scale of measurements or the distance from the source (where the solute is injected into the solvent in the porous medium). This scale-dependent dispersion is called *anomalous*. Arya et al. (1988) suggested that $\alpha \simeq 0.75$. Neuman (1990) presented a different analysis of these and other data, and proposed that there are in fact *two* distinct regimes. The first one is for $L_m \ll 100$ m for which $\alpha \simeq 1.5$, while the second regime, which is relevant to our work, is for $L \gg 100$ m for which α was close to unity. Equation 16 is reminiscent of transport in percolation networks for length scales $L \ll \xi$ (see Eq. 9), and indicates that percolation, fractals, and long-range correlations may have something to do with this scale-dependence of D_L and α_L.

Scale-dependence of α_L implies that it is also *time-dependent*. Hewett (1986), Philip (1986), Arya et al. (1988), Ababou and Gelhar (1990), and Neuman (1990), who studied dispersion in heterogeneous porous media, all used the following equation:

$$\alpha_L \sim t^{\zeta} \tag{17}$$

where a *nonuniversal* $\zeta \simeq 0.5$-0.6 was found to provide reasonably accurate fits of various data. Finally, all of the field-scale data suggest that D_L depends linearly on the average flow velocity v. Although various authors have attempted to explain these data, in our opinion none of these explanations is satisfactory. We note that Koch and Brady (1988) have shown that if the correlation length ξ_k of the permeability heterogeneities is finite, then dispersion is Gaussian and is described by the usual CDE, but if ξ_k is infinite, then:

$$D_L \sim t^{\chi}. \tag{18}$$

However, the χ and ζ that they calculated were universal, and did not depend on the structure of the permeability distribution.

As discussed above, if the permeabilities are distributed according to an fBm, then the pore space must contain regions of very low permeabilities. Elimination of these low permeabilities gives rise to the correlated percolation structure described above. However, as Figure 5 indicates, the resulting percolation structure is nearly the backbone of the system. Therefore, since there are so few stagnant regions in the system, molecular diffusion that transfers the solute into and out of such regions plays no significant role. Its only role is to transfer the solute out of the slow boundary layer zones near the pore surfaces. This means that dispersion of the solute is dominated by mechanical dispersion, a result of the stochastic velocity field imposed on the medium by the permeability distribution. As a result, D_L depends on the average flow velocity v as:

$$D_L \sim \alpha_L \mathrm{v} \tag{19}$$

in agreement with the field data. The effect of diffusion out of the boundary layer zones appears only as a logarithmic correction to Eq. 19. That is, if we include this effect, we obtain (Saffman, 1959; Koch and Brady, 1985) $D_L \sim \alpha_L \mathrm{v} \ln(a\mathrm{v})$, where a is a constant, but since we are interested only in the *scaling* of D_L and α_L with t (or L), such logarithmic corrections do not affect the scaling (because logarithmic corrections are equivalent to *zero* critical exponents, since $\ln(x)$ grows with x slower than any power of x). Note that had diffusion into and out of the stagnant zones been important, we would have had a quadratic dependence of D_L on v, contradicting the field data. We return to this point shortly.

Let us now analyze dispersion in the backbone of the correlated percolation cluster. Although dispersion in random percolation networks has been studied before (Sahimi, 1987; Sahimi and Imdakm, 1988; Koplik et al., 1988), it has not been analyzed in the backbone of the sample-spanning cluster with long-range correlations. Since flow and dispersion take place essentially in the backbone of a percolation structure, the average flow velocity v is proportional to K/X^B. Near p_c scaling laws Eq. 5 and Eq. 7 are valid, and therefore:

$$\mathrm{v} \sim (p-p_c)^{e-\beta_B} \sim \xi^{-\theta_k} \tag{20}$$

where $\theta_k = (e-\beta_B)/\nu = \hat{e} + d_b - d$. Since the permeability correlation length ξ_k is infinite, the only dominant length scale of the system is its linear size L. As a result, the percolation backbone generated by the correlated process is a fractal object, implying that Eq. 20 should be rewritten as:

$$\mathrm{v} \sim L^{-\theta_k}. \tag{21}$$

On the other hand, because L is the only dominant length scale of the system, all other length scales of the system have to be proportional to it. This implies that:

$$\alpha_L \sim L \tag{22}$$

that is, $\alpha = 1$. Thus, combining Eqs. 19, 21 and 22 yields:

$$D_L \sim L^{1-\theta_k}. \tag{23}$$

We take x to be the direction of macroscopic flow, and define $\langle \Delta x^2 \rangle = \langle [x - \langle x \rangle]^2 \rangle = \langle x^2 \rangle - \langle x \rangle^2$, where $\langle \cdot \rangle$ represents an average over all values of x. In general:

$$\langle \Delta x^2 \rangle \sim t^{\zeta'} \tag{24}$$

where $\zeta' = 1$ for Fickian dispersion. Equation 23 is now rewritten as:

$$D_L \sim \langle \Delta x^2 \rangle^{(1-\theta_k)/2}. \tag{25}$$

A fundamental property of diffusion processes tells us that:

$$D_L \sim \frac{d\langle \Delta x^2 \rangle}{dt}. \tag{26}$$

Thus, combining Eqs. 25 and 26 yields, $d\langle \Delta x^2 \rangle / dt \sim \langle \Delta x^2 \rangle^{(1-\theta_k)/2}$, which, after a simple integration, yields:

$$\langle \Delta x^2 \rangle \sim t^{2/(1+\theta_k)} \tag{27}$$

that is, $\zeta' = 2/(1+\theta_k)$. Equation 27 also implies that:

$$D_L \sim t^{(1-\theta_k)/(1+\theta_k)} \tag{28}$$

which means that $\chi = (1-\theta_k)/(1+\theta_k)$. On the other hand, Eq. 21 can be rewritten as $v \sim \langle x \rangle^{-\theta_k}$, and since $v = d\langle x \rangle/dt$, we obtain:

$$\langle x \rangle \sim t^{1/(1+\theta_k)}. \tag{29}$$

Equation 29 should be compared with $\langle x \rangle = vt \sim t$ (v is constant), valid for dispersion in macroscopically homogeneous media. Equation 29 then implies that:

$$v \sim t^{-\theta_k/(1+\theta_k)} \tag{30}$$

which is in sharp contrast with a constant average flow velocity for flow in homogeneous media. Finally, since $\alpha_L = D_L/v$, we combine Eqs. 29 and 30 to obtain:

$$\alpha_L \sim t^{1/(1+\theta_k)} \tag{31}$$

implying that $\zeta = 1/(1+\theta_k)$.

As discussed above, flow and dispersion in heterogeneous porous media take place in the backbone of a percolation cluster with long-range correlations, and the critical exponents that characterize this percolation model are nonuniversal and depend on H. This implies that the exponents χ, ζ and ζ' are also nonuniversal, in agreement with the field data discussed above. We argue that it is in fact the *two-dimensional* correlated percolation that is relevant to the field data, since these data have been obtained at large distances from the source (up to several tens of kilometers), whereas the thickness of such porous media through which the fluids flow is at most a few hundred meters, and therefore such porous media are long and thin, and thus essentially 2-D. Using our results for the critical exponents of the 2-D correlated percolation mentioned above, we find that $0.53 \le \zeta \le 0.62$ for $1/2 \le H < 1$, consistent with the field data that indicate that $\zeta \simeq 0.5$–0.6. Moreover, we find that $1.06 \le \zeta' \le 1.24$, which means that $\langle \Delta x^2 \rangle$ increases with t faster than linearly. This is called *superdiffusion* (Sahimi, 1987). For Fickian dispersion $\zeta' = 1$.

We now investigate briefly the consequences of dispersion in the sample-spanning cluster with a significant fraction of stagnant regions. In this case, D_L depends quadratically on v (Koch and Brady, 1985), and near p_c one has (de Gennes, 1983), $D_L \sim \xi^2 v^2/D$. Moreover, $v \sim K/X^A \sim \xi^{-\theta_a}$, where $\theta_a = (e-\beta)/\nu = \hat{e} + d_p - d$, and therefore $D_L \sim \xi^{2-\theta_a+\theta_d}$. Using the scaling analysis presented above, we find that $\zeta = (2+\theta_d)/[(1+\theta_a)(2\theta_a-\theta_d)]$, $\zeta' = 2/(2\theta_a-\theta_d)$, and $\chi = (2-2\theta_a+\theta_d)/(2\theta_a-\theta_d)$. These results mean, for example, that $\zeta(H=0.6) \simeq 2.06$, in disagreement with the field data and confirming our assertion that it is the backbone of the correlated cluster that is relevant to dispersion in heterogeneous porous media and aquifers. Neither of these results can be obtained by analyzing the CDE. We thus propose that percolation with long-range correlation provides a rational explanation for field-scale experimental data on dispersion coefficients and dispersivities.

Miscible Displacements in Heterogeneous Porous Media

Hydrodynamic dispersion represents the unsteady mixing of two miscible flowing fluids. If the viscosity of the two fluids are not equal, then we have a displacement process in which the solute displaces the solvent. If the viscosity η_1 of the displacing fluid is less than the viscosity η_2 of the displaced fluid, then we have the phenomenon of viscous fingering (Homsy, 1987; Sahimi, 1993b). Due to this viscosity contrast, the front between the two fluids is unstable against small perturbations, and after some time it takes on a fingered configuration. Since miscible displacements are used for enhancing oil production from underground reservoirs, viscous fingering can have serious consequences, because it leaves behind a large amount of oil and makes the displacement process very inefficient. For this reason, viscous fingering has been studied for a long time, both experimentally and theoretically.

However, most studies of viscous fingering in miscible displacements have been restricted to porous media that contain only small-scale heterogeneities with no long-range correlations. Therefore, just as in the case of hydrodynamic dispersion discussed above (the limit $\eta_1 = \eta_2$), it is natural to study miscible displacements in a porous medium in which the permeability varies spatially according to an fBm. Tan and Homsy (1992) studied the effect of permeability correlations on miscible displacement, but their model and method are completely different from what we discuss here.

We used a 760×256 network as the model of the pore space, in which each bond represents a region of the rock to which we assign a permeability that follows an fBm. Assuming that Darcy's law:

$$v = -\frac{K}{\eta} \nabla P \tag{32}$$

describes the flow, where P is the pressure, then for each fluid region we have:

$$\nabla \cdot \left(\frac{K_i}{\eta_i} \nabla P_i \right) = 0 \tag{33}$$

where P_i is the pressure in the fluid region i whose viscosity is η_i, and $i = 1$ and 2. The concentration of each fluid obeys a CDE, Eq. 1. We first ignore dispersion effects, and thus the concentration C_i of each fluid obeys $\partial C_i/\partial t + v_i \cdot \nabla C_i = 0$. In the limit of long times, the governing equation for the concentrations reduces to $\nabla C_i = 0$, that is, the concentration of each fluid in its own region is constant, and therefore the viscosity of the swept region does not depend on the concentrations of the solute and the solvent (with dispersion present, the viscosity of the swept region where the fluids are mixed does depend on the concentrations; see below).

If both η_1 and η_2 are finite, then Eq. 33 has to be solved in both fluid regions, whereas if the displacing fluid is inviscid ($\eta_1 = 0$), then Eq. 33 needs to be solved only for the displaced fluid region, since in this case the pressure in the displacing fluid region is constant. In both cases the front between the two fluids advances according to Darcy's law. Let $M = \eta_2/\eta_1$ be the viscosity ratio. Since Eq. 33 is a randomized Laplace equation, it can be solved by a random walk method. If $M = \infty$,

then the random walk algorithm for solving Eq. 33 and simulating a miscible displacement in this limit is as follows (Paterson, 1987). Suppose that Δx_1 and Δx_2 are the step lengths of a random walker in two zones with permeabilities K_1 and K_2. Then $\Delta x_1/\Delta x_2 = K_1/K_2$, that is, in a unit of time the random walker takes a larger step in the high permeability zone or, if the step lengths are taken to be equal, the walker explores the high permeability zone for a longer period of time (the front between the two fluids advances in the high permeability zone more often). Therefore, one starts with a square network filled by the fluid to be displaced, except for one boundary row of the network which is filled by the displacing fluid. This represents the beginning of the simulations, corresponding to the beginning of the actual experiment, when the displacing fluid has just been injected into the medium. Since for $M=\infty$ one has to solve Eq. 33 only in the displaced fluid region, random walkers are released into the system at the face opposite to the injection line. They perform a random walk in the displaced fluid zone, selecting a direction at each site of the network with a probability proportional to the permeability of the bond in that direction. If a random walker arrives at a node which is adjacent to the front, then that node and the bond connecting it to the front are also occupied by the displacing fluid (since the flux of such particles obeys Darcy's law, which is the speed with which the front advances). The random walker is removed from the system, and another random walker is injected into the system. The simulation continues until the front reaches the opposite boundary of the system, that is, the breakthrough point.

The random walk algorithm for finite values of M is as follows (Siddiqui and Sahimi, 1990). One uses *two* random walkers, one for each fluid region, since in this case Eq. 33 has to be solved for *both* regions of displaced and displacing fluids. Thus, the random walkers are injected into their corresponding regions and perform their random walks as before. Once they arrive in the vicinity of the front, they advance it with probabilities p_1 and p_2, corresponding respectively to the displacing and displaced fluid regions. The equations for p_1 and p_2 that relate them to the viscosities of the fluids and the permeability distribution are derived using the fact that the pressure and the fluid velocity are continuous across the front (Siddiqui and Sahimi, 1990). Thus, if a random walker is in the displacing fluid region in the vicinity of the front, it advances it with a probability $p_1 = 1/(\lambda+1)$, whereas a random walker in the displaced fluid region advances the front with probability $p_2 = \lambda/(\lambda+1)$, where $\lambda = \lambda_1/\lambda_2$ and $\lambda_i = K_i/\eta_i$ is the mobility of fluid i. In this case, $\Delta x_1/\Delta x_2 = \lambda = MK_1/K_2$. The advantage of this random walk algorithm is that it allows us to use very large systems, which are essential for simulating heterogeneous media, since the equations are solved only implicitly. We carried out our simulations for various values of M, averaging the results for each M over 10 different realizations of the network.

Experiments and simulations of miscible displacements in *homogeneous* porous media both indicate (Homsy, 1987; Sahimi, 1993b) that the areal sweep efficiency of the process, that is, the areal fraction of the zones swept by the displacing fluid, depends strongly on M and varies by about one order of magnitude, as M is varied between $M=1$ and $M=100$. Moreover, the displacement patterns are also controlled by M. In contrast, for miscible displacements in heterogeneous porous media with long-range correlations simulated here M has virtually no effect. Figure 7 shows the displacement patterns with $H=0.75$ for $M=\infty$ and $M=4$, and as can be seen the two patterns are virtually identical. Figure 8 shows the dependence of the areal sweep efficiency on M and, except for M close to unity, the sweep efficiency is essentially independent of M. To understand these results we resort to the distribution of the permeabilities shown in Figure 9. The permeabilities at the central region of the system are much lower than those on the sides, which form the backbone of the cluster in which the displacement takes place. Therefore, the most important factor is the competition between the two high permeability zones, which in this case is won by the left side.

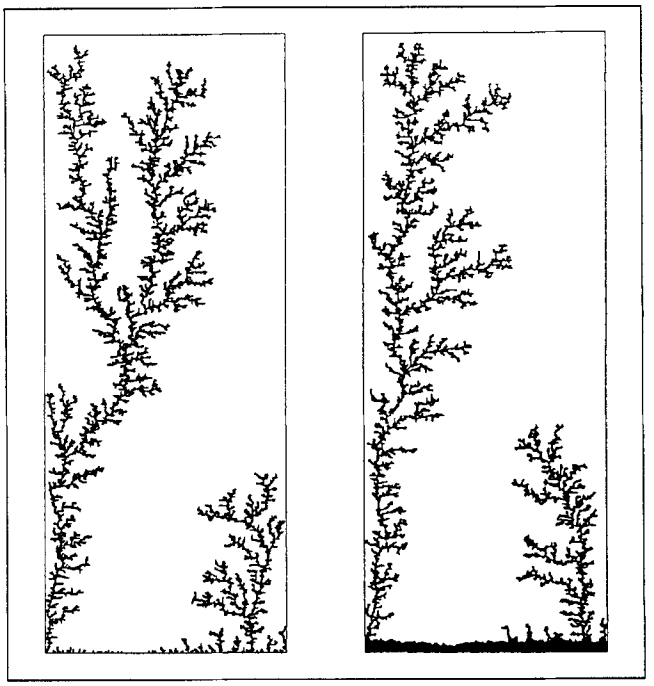

Figure 7. Displacement patterns for $M=\infty$ (left) and $M=4$ (right) in a 2-D porous medium in which the permeabilities are distributed according to an fBm with $H=0.75$.

The case in which dispersion effects are not ignored is more complex, since the viscosity of the mixed zone depends on the viscosities of both displacing and displaced fluids, and thus the complete problem is nonlinear. The CDE has to be solved for both displacing and displaced regions, coupled with a mixing law for the viscosity of the mixed zone that relates it to the viscosities (or concentrations) of the two fluids. A random walk algorithm for this case is as follows. At each time step, one calculates the flow field throughout the system. This is straightforward, as Darcy's law is applicable, and therefore the equations for the pressure field are linear. Similar to the case of no dispersion, fluid particles (random walkers) that carry a finite concentration of the displacing fluid are injected into the system and are moved with velocities based on the pressure field. This simulates the effect of convection. The particle velocities are calculated at the midpoint between pressure nodes. After moving the particles to their current positions, the effect of dispersion is simulated by randomly perturbing the particle

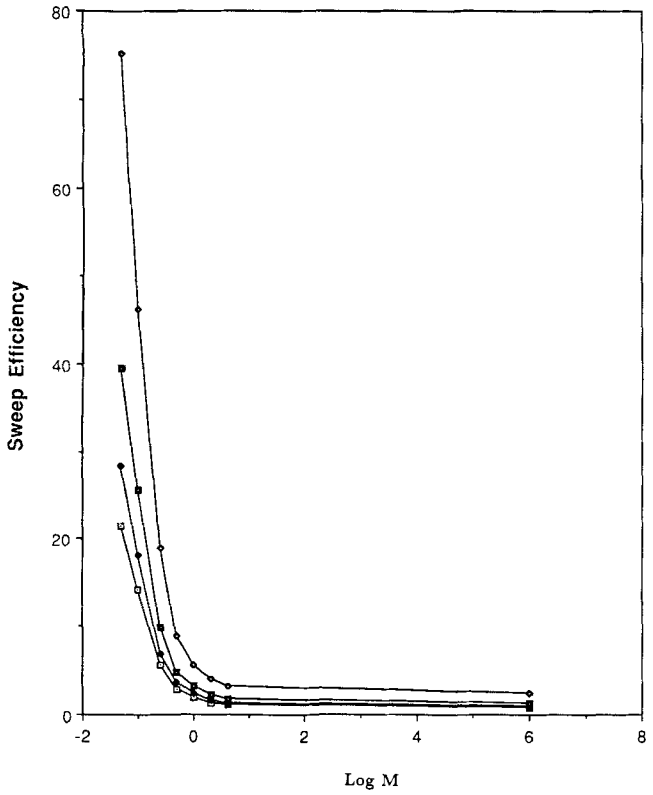

Figure 8. Dependence of the sweep efficiency on the mobility ratio *M* for the porous medium of Figure 7.

The results are, from top to bottom, for one, two, three, and four orders of magnitude variations in the permeabilities.

positions in the longitudinal and transverse directions by two distances proportional to $\ell_L = r(2D_L t)^{1/2}$ and $\ell_T = r(2D_T t)^{1/2}$, where r is a random number uniformly distributed in (0,1). The new pressure field is calculated, the new positions of the particles are determined, and so on. The main disadvantages of this method are that one has to have *a priori* estimates of D_L and D_T, and that computations are very intensive, as the pressure field has to be constantly updated. This method was originally developed by Smith and Schwartz (1980) for the $M = 1$ case and by Araktingi and Orr (1988) for an arbitrary value of M. We used this method in which the permeabilities were

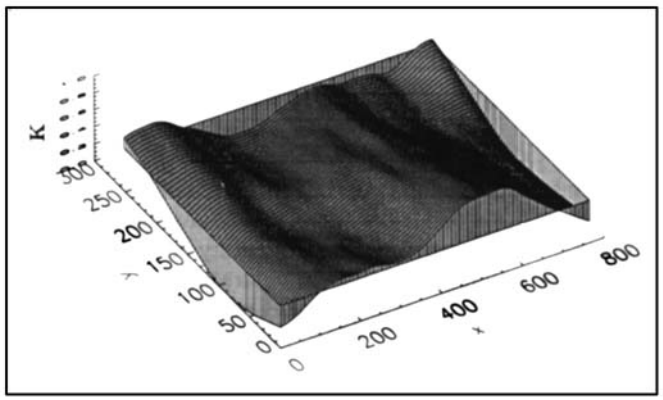

Figure 9. 3-D permeability distribution for the porous medium of Figure 8.

distributed according to a fBm with $H = 0.75$, with $D_L = 0.1457$ ft^2/day and $D_T = 0.0045$ ft^2/day, given by Araktingi and Orr (1988). We found our results to be qualitatively very similar to Figures 7 and 8, thus confirming the generality of our results.

These results show that conventional viscous fingers, which are the result of the viscosity contrast between the displacing and displaced fluids, *do not exist* in a field-scale miscible displacement in a heterogeneous porous medium with long-range correlations. That is, viscous fingers are the creation of small-scale and homogeneous porous media used in laboratory experiments, and do not exist outside the laboratory. Although there is similarity between the displacement patterns shown in Figure 7 and those obtained in homogeneous porous media, the similarity is superficial: One is the result of long-range correlations in the structure of the medium, while the other is the product of the viscosity contrast between the displacing and displaced fluids. We should emphasize that if we introduce a cutoff ξ_{co} in the fBm, then at large enough length scales the behavior of the displacement would be similar to those in homogeneous porous media. Elsewhere, we have shown (Lauritsen et al., 1993) how the effect of long-range correlations represented by an fBm can dramatically change the nature of nonequilibrium growth processes such as aggregation phenomena. Thus, once again, long-range correlations and the formation of sample-spanning high permeability paths completely control our phenomenon, giving rise to effects that are absent in a random system. We also studied (Sahimi and Knackstedt, 1994) the effect of stratification on viscous fingering with long-range correlations and reached similar conclusions.

Continuum Percolation and Transport in Random Flow Fields

We now discuss percolation in random continua (for a review of continuum percolation see Balberg (1987)). There are several models of percolating continua. One can, for example, insert at random circular or spherical inclusions in an otherwise homogeneous medium, and obtain the so-called *swiss-cheese* model. This model has in fact been used by chemical engineers for modeling gas-solid reactions and combustion (Sahimi et al., 1990). Several other models of continuum percolation have been developed and used for various linear (Balberg, 1987) and nonlinear transport processes (Sahimi, 1993a) in disordered media. But let us discuss a particular model of continuum percolation that is directly relevant to this article.

In this continuum percolation model, called the *potential model*, a smooth random function $\psi(\mathbf{r})$ is considered. A percolation cluster is constructed by considering those regions of space for which $\psi(\mathbf{r}) \leq h$, where h is a constant. This model was first suggested by Ziman (1969) and Zallen and Scher (1971) who were interested in electron localization in disordered media. In their model $\psi(\mathbf{r})$ represents the potential, or energy barrier, that is created by the disordered regions of the system, and h is the energy of an electron. Thus, if $h \geq \psi(\mathbf{r})$, then the electron can pass through this region of the system. Therefore, there must be a critical value h_c of h, such that for $h_c \geq \psi(\mathbf{r})$ a sample-spanning region can form in which the electrons can flow, and thus the disordered system can conduct.

To make a clear connection between this model and dispersion of a passive particle in a random flow field that we want to study here, we use the analogy that was originally suggested by Zallen and Scher (1971). We consider a *flooded*

landscape and a 2-D random function $\psi(x, y)$, where ψ represents the shape of the earth relief and h denotes the water level. Thus, $\psi(x, y) \le h$ describes those areas that are flooded. For $h \ll h_c$, one has only small lakes and the rest of the land is dry. As $h \to h_c$ larger and larger lakes are formed that become connected together and give rise to large flooded areas. At $h = h_c$ a sample-spanning flooded area is formed. Since the system that we consider is two-dimensional, it is impossible to simultaneously have sample-spanning dry and flooded areas. Therefore, at $h = h_c$ an infinite or a sample-spanning *coastline* exists, which is nothing but a contour of the function $\psi(x, y)$ that envelops the sample-spanning cluster. Given the definition of the percolation hulls given above, it should be obvious that this contour is just the hull of the sample-spanning percolation cluster at $h = h_c$, the percolation threshold of the system. Since we have not put any restriction on the admissible forms of $\psi(x, y)$ (aside from the usual differentiability requirement), it should be clear that *any* such function can generate the hull. Thus, if ψ represents a stream function, then dispersion of a passive particle in the incompressible flow field generated by such a function represents transport *around* a sample-spanning percolation cluster. Thus, although the connection between transport in such random flow fields and percolation may not be obvious at the first sight, the definition of the hull of percolation clusters and its construction for *continuum percolation* establishes this connection. The topological exponents of continuum and network percolation are the same, and therefore the fractal dimension d_h of the hull generated by $\psi(x, y)$ is $d_h(d=2) = 7/4$ (see Table 1). We now use this connection and study transport of a passive particle in a 2-D incompressible random flow field. This problem is relevant to a wide variety of phenomena, such as 2-D rolls of the Rayleigh-Bénard problem, Taylor vortices in Couette flow, weakly unstable magnetohydrodynamic instabilities, and the generation of a magnetic field from the passive convection of a magnetic flux.

We assume that molecular diffusion is not negligible. Transport then is described by a CDE. We define a Péclet number $Pe = Lv/D_m$, where L is an appropriate length scale of the system, and D_m is the molecular diffusivity. As is well-known, the effective longitudinal dispersion coefficient D_L of the system scales with Pe as:

$$\frac{D_L}{D_m} \sim Pe^{\gamma}. \tag{34}$$

The limit $\gamma = 2$ corresponds to the classical Taylor-Aris dispersion (Taylor, 1953; Aris, 1956) in a capillary tube, or dispersion in a porous medium with significant regions of stagnant fluid (Koch and Brady, 1985). Rosenbluth et al. (1987) considered this problem in 2-D incompressible flows in periodic rolls with periodicities w_x and w_y, and the stream function $\psi(x, y)$ was taken to be:

$$\psi(x, y) = \psi_0 \sin\left(\frac{\pi x}{w_x}\right) \sin\left(\frac{\pi y}{w_y}\right) \tag{35}$$

where ψ_0 is a constant. Rosenbluth et al. (1987) developed an asymptotic method for large values of Pe and showed that $\gamma = 1/2$. A similar result was also obtained by Moffat (1983), Sagues and Horsthemke (1986), Perkins and Zweibel (1987), and Shraiman (1987) using various numerical methods. Nadim et al. (1986) considered the more complex problem of transport in concentrated suspensions of a periodic set of rotating cylinders, and showed by numerical simulations that the dominant form of contribution to D_L is described by Eq. 34 with $\gamma = 1/2$ again. Here we assume that $\psi(x, y)$ is an isotropic oscillating function characterized by a wavelength w and an amplitude $|\psi| \sim \psi_0 \sim wv$. We also take $\langle \psi \rangle = 0$, so that $h_c = \langle \psi \rangle = 0$ as well.

As discussed above, the contours of stream functions represent the hull of 2-D percolation clusters. Thus, the typical transverse distance ℓ_c between the streamlines $\psi(x, y) = h$ should diverge as $h \to h_c = 0$ according to the power law:

$$\ell_c \sim \left(\frac{\psi - \psi_c}{h}\right)^{\nu} \tag{36}$$

since ℓ_c should be proportional to the typical radius of the cluster whose hull is formed by the contours of the stream function, and therefore it should be proportional to the correlation length of percolation defined above. Here $\psi_c = 0$ represents the critical value of ψ at h_c. Given our assumptions about the structure of the stream function $\psi(x, y)$, Eq. 36 is rewritten as:

$$\ell_c \sim \left(\frac{\psi_0}{h}\right)^{\nu}. \tag{37}$$

Almost all streamlines of an isotropic flow are closed. Therefore, the length ℓ_h of a closed streamline is similar to the hull of the percolation cluster, and therefore we can write:

$$\ell_h \sim \left(\frac{\ell_c}{w}\right)^{d_h} \tag{38}$$

which, after using Eq. 37, is rewritten as:

$$\ell_h \sim \left(\frac{\psi_0}{h}\right)^{\nu d_h}. \tag{39}$$

We consider the limit in which the Péclet number $Pe = Lv/D_m \sim \psi_0/D_m$ is large, so that the main effect of molecular diffusion manifests itself only in a diffusive boundary layer in the slow regions of the flow field. The thickness δ of this boundary layer is of the order of:

$$\delta \sim \left(\frac{D_m \ell_h}{v}\right)^{1/2}. \tag{40}$$

To make contact with the system that Rosenbluth et al. and other studied, we divide the system into convection cells with a diameter of the order of ℓ_c and a density N_c per unit area. Here a convection cell is a bundle of streamlines which share a common portion whose width is $w_c \sim wh/\psi_0$. Clearly, we have $N_c \sim \ell_c^2$, as such cells fill the system. To calculate D_L we determine the flux J of the particles. Since the system contains convection cells in a random flow field, we have to average J over such cells. Therefore, if C is the concentration of the particles, the average $\langle J \rangle$ is given by:

$$\langle J\rangle = -\int_{h_l}^{h_u} (N_c \ell_c \ell_h)\,(v\ell_c/\ell_h)\,(\delta/h)\,\nabla C dh. \qquad (41)$$

In writing this equation we observed that the quantity $v\ell_c/\ell_h$ is the velocity component in the direction of ∇C, and δ/h is the area fraction responsible for transport. Clearly, the upper limit of the integral is $h_u = \infty$. However, the lower limit h_l should be chosen with care since, if we take $h_l = 0$ (that is, infinitely large convection cells), the integral (Eq. 41) will diverge. To estimate h_l, we consider the fact that the thickness δ of the diffusive boundary layer has to be small, because otherwise no convection cell can contain this boundary layer. Thus, we argue that δ is at most of the order of $w_c \sim wh/\psi_0$, the width of the portion that the bundle of the streamlines share in a cell, and therefore h_l is the solution of the equation $\delta = w_c$. Using Eq. 40 then yields, $h_l = \psi_0 Pe^{-1/(2+\nu d_h)}$, which together with Eqs. 37 and 39 for ℓ_c and ℓ_h enable us to carry out the integration in Eq. 41. The result, when compared with $\langle J\rangle = -D_L \nabla C$ yields:

$$\frac{D_L}{D_m} \sim Pe^{(1+\nu d_h)/(2+\nu d_h)} \sim Pe^{(2+\nu)/(3+\nu)} \qquad (42)$$

where we used Eq. 4 for 2-D percolation. The fact that γ can be expressed in terms of the exponent ν of percolation indicates the usefulness and power of percolation concepts. Using $\nu = 4/3$ for 2-D percolation, we find that $\gamma = 10/13 \simeq 0.77$, larger than $\gamma = 1/2$ found by Rosenbluth et al. (1987) and others. The reason for this is that the stream function (Eq. 35) considered by Rosenbluth et al. gives rise to an *unstable* system, in the sense that a small perturbation in the flow field generates streamlines that are of infinite extent, thereby destroying the periodic and cellular structure that they studied. Thus, the system that these authors studied is actually the most unfavorable for transport of the particles, and thus $\gamma = 1/2$ is the lowest value that one can obtain. Equation 42 demonstrates once again the role of percolation, and the long-range correlations that fractality of the percolation hull induces in transport phenomena in a disordered medium.

Conclusion

Using percolation, fractal, and scaling concepts, as well as Monte Carlo simulations, we studied three types of transport processes in disordered media which at microscales are all described by a convective-diffusion equation. Our results clearly demonstrate that the interplay between the correlated nature of the structure of the media and the transport process can give rise to a rich variety of macroscopic transport regimes that are absent from uncorrelated systems. We hope that our results will stimulate more work in this rich and important area of research.

Acknowledgments

This article was prepared while I was visiting the HLRZ-KFA Supercomputer Center in Jülich, Germany. I am grateful to the Center and Hans Herrmann for warm hospitality. I would also like to thank Sumit Mukhopadhyay and Mark Knackstedt for their help in some of the computations. While this article was being proofread, we became aware that Sichinko and Kalda (*J. Nonlinear Sci.*, **1**, 375, 1991) derived an equation similar to Eq. 42 in the context of magnetic fluxes in disordered solids.

Notation

d = Euclidean dimensionality
d_b = fractal dimension of the backbone
d_h = fractal dimension of the hull
d_p = fractal dimension of the sample-spanning cluster
D = macroscopic diffusivity
e = permeability exponent
f = conductance or permeability distribution
g = bond conductance
G = effective conductivity of a network
H = parameter of fBm
M = viscosity ratio
N_c = density of convection cells
p = conducting fraction of the system
t = time
X^A = accessible fraction
w = wavelength

Greek letters

α = length scale exponent of dispersivity
α_L = longitudinal dispersivity
β = exponent of accessible fraction
β_B = exponent of backbone fraction
γ = Péclet number exponent
δ = boundary layer thickness
ζ = time exponent of dispersivity
ζ' = exponent of mean square displacement
η = fluid viscosity
λ = fluid mobility
μ = conductivity exponent
ν = correlation length exponent
ξ_{co} = cutoff length scale
χ = time exponent of D_L
ψ = stream function

Literature Cited

Ababou, R., and L. W. Gelhar, in *Dynamics of Fluids in Hierarchical Porous Media*, J. H. Cushman, ed., Academic Press, London (1990).
Araktingi, U. G., and F. M. Orr, Jr., "Viscous Fingering in Heterogeneous Porous Media," SPE Paper 18095, Houston (1988).
Aris, R., "On the Dispersion of a Solute in a Fluid Flowing Through a Tube," *Proc. Roy. Soc. London*, **A235**, 67 (1956).
Arya, A., T. A. Hewett, R. G. Larson, and L. W. Lake, "Dispersion and Reservoir Heterogeneity," *SPE Reservoir Eng.*, **3**, 139 (1988).
Balberg, I., "Recent Developments in Continuum Percolation," *Philos. Mag.*, **B56**, 991 (1987).
de Gennes, P. G., "Hydrodynamic Dispersion in Unsaturated Porous Media," *J. Fluid Mech.*, **136**, 189 (1983).
Feng, S., B. I. Halperin, and P. N. Sen, "Transport Properties of Continuum Systems near the Percolation Threshold," *Phys. Rev.*, **B35**, 197 (1987).
Gelhar, L. W., C. Welty, and K. R. Rehfelt, "A Critical Review of Data on Field-Scale Dispersion in Aquifers," *Water Res. Res.*, **28**, 1955 (1992).
Hewett, T. A., "Fractal Distributions of Reservoir Heterogeneity and their Influence on Fluid Transport," SPE Paper 15386, New Orleans (1986).
Hewett, T A., and R. A. Behrens, "Conditional Simulation of Reservoir Heterogeneity with Fractals," *SPE Form. Eval.*, **5**, 217 (1990).
Homsy, G. M., "Viscous Fingering in Porous Media," *Ann. Rev. Fluid Mech.*, **19**, 271 (1987).
Koch, D. L., and J. F. Brady, "Dispersion in Packed Beds," *J. Fluid Mech.*, **154**, 399 (1985).
Koch, D. L., and J. F. Brady, "Anomalous Diffusion in Heterogeneous Porous Media," *Phys. Fluids*, **31**, 965 (1988).
Kogut, P. M., and J. P. Straley, "Distribution-Induced Non-universality of the Percolation Conductivity Exponent," *J. Phys. C*, **12**, 2151 (1978).
Koplik, J., S. Redner, and D. Wilkinson, "Transport and Dispersion in Random Networks with Percolation Disorder," *Phys. Rev.*, **A37**, 2619 (1988).

Lauritsen, K. B., M. Sahimi, and H. J. Herrmann, "Effect of Quenched and Correlated Disorder on Growth Phenomena," *Phys Rev.*, **E48**, 1272 (1993).
Mandelbrot, B. B., and J. W. Van Ness, "Fractional Brownian Motion, Fractional Noises and Applications," *SIAM Rev.*, **10**, 422 (1968).
Moffatt, H. K., "Transport Effects Associated with Turbulence with Particular Attention to the Influence of Helicity," *Rep. Prog. Phys.*, **46**, 621 (1983).
Nadim, A., R. G. Cox, and H. Brenner, "Taylor Dispersion in Concentrated Suspensions of Rotating Cylinders," *J. Fluid Mech.*, **164**, 185 (1986).
Neuman, S. P., "Universal Scaling of Hydraulic Conductivities and Dispersivities in Geologic Media," *Water Res. Res.*, **26**, 887 (1990).
Paterson, L., "Simulations of Fluid Displacement in Heterogeneous Porous Media," *J. Phys. A*, **20**, 2179 (1987).
Peng, C.-K., J. Mietus, J. M. Hausdorff, S. Havlin, H. E. Stanley, and A. L. Goldberg, "Long-range Anticorrelation and Non-Gaussian Behavior of Heartbeat," *Phys. Rev. Lett.*, **70**, 1343 (1993).
Perkins, F. W., and E. G. Zwiebel, "A High Magnetic Reynolds Number Dynamo," *Phys. Fluids*, **30**, 1079 (1987).
Philip, J. R., "Issues in Flow and Transport in Heterogeneous Porous Media," *Transp. Porous Media*, **1**, 319 (1986).
Prakash, S., S. Havlin, M. Schwartz, and H. E. Stanley, "Structural and Dynamical Properties of Long-range Correlated Percolation," *Phys. Rev.*, **A46**, R1724 (1992).
Rosenbluth, M. N., H. L. Berk, I. Doxas, and W. Horton, "Effective Diffusion in Laminar Convective Flows," *Phys. Fluids*, **30**, 2636 (1987).
Saffman, P. G., "A Theory of Dispersion in a Porous Medium," *J. Fluid Mech.*, **6**, 321 (1959).
Sagues, F., and W. Horsthemke, "Diffusive Transport in Spatially Periodic Hydrodynamic Flows," *Phys. Rev.*, **A34**, 4136 (1986).
Sahimi, M., "Hydrodynamic Dispersion near the Percolation Threshold: Scaling and Probability Densities," *J. Phys. A*, **20**, L1293 (1987).
Sahimi, M., "Nonlinear Transport Processes in Disordered Media," *AIChE J.*, **39**, 369 (1993a).
Sahimi, M., "Flow Phenomena in Rocks: From Continuum Models to Fractals, Percolation, Cellular Automata and Simulated Annealing," *Rev. Mod. Phys.*, **65**, 1393 (1994).
Sahimi, M., *Applications of Percolation Theory*, Taylor and Francis, London (1994).
Sahimi, M., G. R. Gavalas, and T. T. Tsotsis, "Statistical and Continuum Models of Fluid-Solid Reactions in Porous Media," *Chem. Eng. Sci.*, **45**, 1443 (1990).
Sahimi, M., B. D. Hughes, L. E. Scriven, and H. T. Davis, "Stochastic Transport in Disordered Systems," *J. Chem. Phys.*, **78**, 6849 (1983).
Sahimi, M., and A. O. Imdakm, "The Effect of Morphological Disorder on Hydrodynamic Dispersion in Flow Through Porous Media," *J. Phys. A*, **21**, 3833 (1988).
Sahimi, M., and M. A. Knackstedt, "No Viscous Fingers in Heterogeneous Porous Media," *J. Phys. I France*, **4**, 1269 (1994).
Sahimi, M., and S. Mukhopadhyay, "Fractional Brownian Motion and Long-Range Percolation," *Phys. Rev. E*, in press (1995).
Saleur, H., and B. Duplantier, "Exact Determination of the Percolation Hull Exponent in Two Dimensions," *Phys. Rev. Lett.*, **58**, 2325 (1987).
Shraiman, B. I., "Diffusive Transport in a Rayleigh-Bénard Convection Cell," *Phys. Rev.*, **A36**, 261 (1987).
Siddiqui, H., and M. Sahimi, "Computer Simulations of Miscible Displacement Processes in Disordered Porous Media," *Chem. Eng. Sci.*, **45**, 163 (1990).
Smith, L., and F. W. Schwartz, "Mass Transport: 1. A Stochastic Analysis of Macroscopic Dispersion," *Water Resour. Res.*, **16**, 303 (1980).
Stauffer, D., and A. Aharony, *Introduction to Percolation Theory*, 2nd ed., Taylor and Francis, London (1992).
Straley, J. P., "Non-universal Threshold Behavior of Random Resistor Networks with Anomalous Distribution of Conductances," *J. Phys. C*, **15**, 2343 (1982).
Strenski, P. N., R. M. Bradley, and J.-M. Debierre, "Scaling Behavior of Percolation Surfaces in Three Dimensions," *Phys. Rev. Lett.*, **66**, 1330 (1991).
Tan, C.-T., and G. M. Homsy, "Viscous Fingering with Permeability Heterogeneity," *Phys. Fluids A*, **4**, 1099 (1992).
Taylor, G. I., "The Dispersion of Soluble Matter in Solvent Flowing Slowly Through a Tube," *Proc. Roy. Soc. London*, **A219**, 186 (1953).
Weinrib, A., "Long-Range Correlated Percolation," *Phys. Rev.*, **B29**, 387 (1984).
Weinrib, A., and B. I. Halperin, "Critical Phenomena in Systems with Long-Range Correlated Quenched Disorder," *Phys. Rev.*, **B27**, 413 (1983).
Zallen, R., and H. Scher, "Percolation on a Continuum and the Localization-Delocalization Transition in Amorphous Semiconductors," *Phys. Rev.*, **B4**, 4471 (1971).
Ziff, R. M., "Test of Scaling Exponents for Percolation Cluster Perimeters," *Phys. Rev. Lett.*, **56**, 545 (1986).
Ziman, J. M., "The Localization of Electrons in Ordered and Disordered Systems: I. Percolation of Classical Particles," *J. Phys. C.*, **1**, 1532 (1969).

Manuscript received Dec. 6, 1993, and revision received Feb. 28, 1994.